Science and Technology of Welding and Joining

ISSN: (Print) (Online) Journal homepage: https://www.tandfonline.com/loi/ystw20

Evaluating susceptibility of Ni-base alloys to solidification cracking by transverse-motion weldability test

Chunzhi Xia & Sindo Kou

To cite this article: Chunzhi Xia & Sindo Kou (2020): Evaluating susceptibility of Ni-base alloys to solidification cracking by transverse-motion weldability test, Science and Technology of Welding and Joining, DOI: 10.1080/13621718.2020.1802897

To link to this article: https://doi.org/10.1080/13621718.2020.1802897

Published online: 05 Aug 2020.

SCIENCE AND TECHNOLOGY OF WELDING AND JOINING
https://doi.org/10.1080/13621718.2020.1802897

The Institute of Materials, Minerals and Mining

Taylor & Francis
Taylor & Francis Group

Evaluating susceptibility of Ni-base alloys to solidification cracking by transverse-motion weldability test

Chunzhi Xia[a] and Sindo Kou[b]

[a]Department of Materials Science and Engineering, Jiangsu University of Science and Technology, Zhenjiang, People's Republic of China; [b]Department of Materials Science and Engineering, The University of Wisconsin, Madison, WI, USA

ABSTRACT

The transverse-motion weldability (TMW) test, in which the lower sheet in lap welding is moved at a constant speed V in the transverse direction of welding to induce solidification cracking, was applied to Ni-base alloys. Alloys 600, 625, 718 and 800 were used as example materials for demonstration. The relative susceptibility ranking of the alloys was similar to those reported. A similar ranking was calculated based on $|dT/d(f_S)^{1/2}|$ near $(f_S)^{1/2} = 1$ (T: temperature; f_S: fraction solid). Based on the transverse micrograph of the weld and V, the critical local strain rate near the crack was estimated. It was significantly higher for 718 than 800, consistent with the significantly lower susceptibility of 718 shown by the TMW test.

ARTICLE HISTORY
Received 21 June 2020
Revised 25 July 2020
Accepted 25 July 2020

KEYWORDS
Solidification cracking; Ni-base alloys; welding; weldability test; transverse-motion weldability test

Introduction

Solidification cracking is known to occur in Al alloys, stainless steels, and Ni-base alloys [1]. Recently, Soysal and Kou [2] developed the transverse-motion weldability (TMW) test for assessing the susceptibility to solidification cracking. As shown in Figure 1(a), lap welding is conducted between a stationary upper sheet and a lower sheet moving in the transverse direction of welding at the speed V. The motion of the lower sheet induces transverse tension in the mushy zone to cause solidification cracking. The upper and lower sheets are connected to each other by the mushy zone (the weld pool has no strength). Since the mushy zone is much weaker and smaller in size than the workpiece, deformation occurs in the mushy zone alone and not in the workpiece. The TMW test was used to assess the solidification cracking susceptibility of Al alloys [1], the effectiveness of Al filler metals in reducing the crack susceptibility [3], and the validity of the prediction of the crack susceptibility [4]. The test has been used primarily for Al alloys [2–5] but also for Mg alloys [6] and stainless steels [7]. Unlike the widely used Varestraint test [8], tension can be induced very slowly as in welding practice, and a filler metal can be used during welding to evaluate its effect of solidification cracking [2,3]. The test is cost effective, requiring only a motor to move the lower sheet and a small amount of the test material.

The main purpose of the present study was to apply the TMW test to Ni-base alloys. Since solidification cracking is a significant issue for Ni-base alloys and since the TMW test is a new test with significant advantages over the Varestraint test, it is desirable to demonstrate the TMW test of Ni-base alloys. The test results were compared with previous experimental results based on other tests and with calculated results of the crack susceptibility. A secondary purpose was to estimate the local strain rate in the mushy zone based on the transverse micrograph of the weld and V.

Experimental procedure

The chemical compositions of the alloys used are given in Table 1. The upper sheet was 25.4 mm by 127 mm by 3.2 mm, and the lower sheet 76.2 mm by 76.2 mm by 3.2 mm. The lower sheet was positioned to stick out beyond the upper sheet by 10 mm before welding. The surface of each sheet near the weld bead was polished to remove oxides and then cleansed with acetone before welding.

Lap welding was conducted by gas tungsten arc welding (GTAW) under the following conditions: welding current at 110 A (DCEN), voltage 10.2 V, Ar gas shielding 3.15×10^{-4} m^3 s^{-1} (40 ft^3 h^{-1}), torch travel speed 1.27 mm s^{-1}, and 3.2 mm diameter tungsten electrode with a 15° tip angle. The same welding conditions were used for testing the crack susceptibility of all alloys. The upper sheet was stationary, and the lower sheet was moved by a servomotor. The moving speed was programmed to start higher at 0.5 mm s^{-1} to ensure crack initiation and then step down to a lower predetermined speed for the rest of the test.

The initial moving speed of the lower sheet needs to be fast enough to initiate solidification cracking in all

CONTACT Sindo Kou kou@engr.wisc.edu

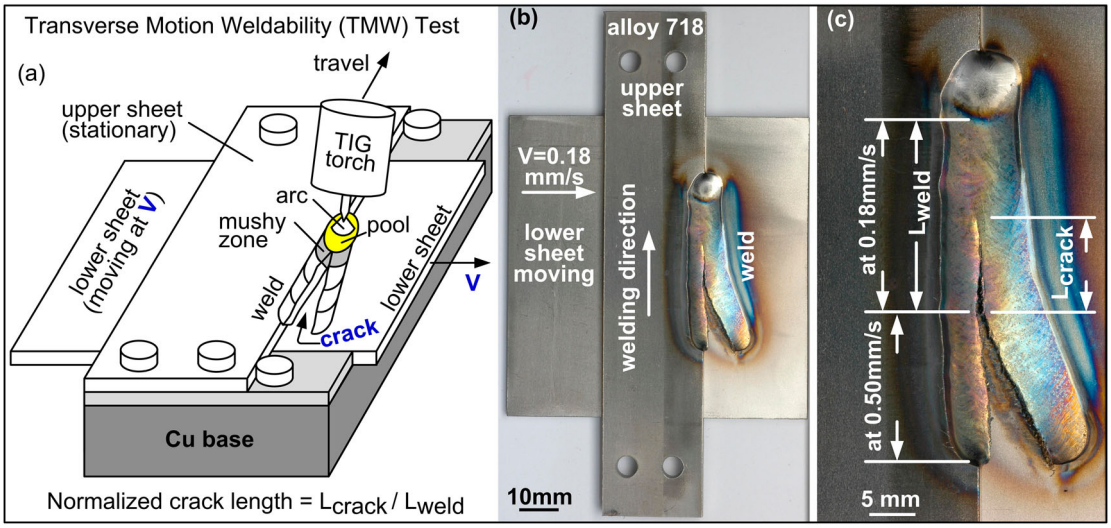

Figure 1. TMW test: (a) schematic [2]; (b) (c) alloy 718 after testing.

Table 1. Chemical compositions of the nickel alloys.

	Chemical composition (wt-%)													
Alloys	C	Mn	P	S	Si	Al	Cu	Ni	Fe	Cr	Mo	Co	Ti	Nb
600	0.05	0.8	–	0.009	0.3	0.23		Bal.	8.0	15.5	0.02	0.049	0.21	–
625	0.04	0.35	0.009	0.0001	0.19	0.21	0.08	Bal.	4.38	22.0	8.40	0.04	0.21	3.44
800	0.04	1.35	0.014	–	0.8	0.3	0.3	32	Bal.	21.0	–	–	0.4	0.065
718	0.059	0.23	0.010	< 0.002	0.09	0.56	0.06	52.8	Bal.	18.3	3.04	0.48	1.03	5.02

the specimens being tested. In the TMW tests by GTAW, 0.7 mm s^{-1} was found fast enough for Al alloys [4] and for stainless steels [7]. In fact, a review of these test results showed 0.5 mm s^{-1} would have been fast enough as well. Thus, in the present study on Ni-base alloys it was decided to use 0.5 mm s^{-1} as the initial speed. For a given alloy the initial speed was dropped from 0.5 mm s^{-1} to a much lower speed, e.g. 0.05 mm s^{-1}. Taking alloy 718 as an example, the crack did not propagate at all at 0.05 mm s^{-1}. A significantly higher speed than 0.05 mm s^{-1}, e.g. 0.2 mm s^{-1} was then tried, and the crack was found to propagate all the way to the weld end. A slightly lower speed of 0.18 mm s^{-1} was then tried, and the crack was found to propagate much less. So, the minimum speed for full crack propagation to the weld end was taken as 0.2 mm s^{-1}.

After welding, the samples were cut in the transverse direction near the tip of the crack and polished. Alloy 600 was etched with Marble's Reagent, i.e. 10 g $CuSO_4$, 50 ml HCl and 50 ml distilled water. Alloy 800 was etched with a mixed acid consisting of equal parts of HCl, HNO_3 and fresh CH_3COOH. As for alloys 625 and 718, they were etched with a mixed acid consisting of 3 ml HNO_3, 5 ml H_2SO_4 and 90 ml HNO_3.

Results and discussion

Crack susceptibility tested

Figure 1(b) shows an example of alloy 718 after the TMW test. The weld is enlarged in Figure 1(c). V was 0.50 mm s^{-1} initially to ensure crack initiation before being stepped down to 0.18 mm s^{-1} for crack propagation. The normalised crack length is taken as L_{crack}/L_{weld}, where L_{crack} is the crack length and L_{weld} the weld length corresponding to the test speed [2–4], which in the present example is 0.18 mm s^{-1}.

The results of the TMW test are shown in Figure 2 by plotting the normalised crack length vs. V. L_{crack}/L_{weld} is initially 0 (no crack) and it rises to 1.0 (full crack) with increasing V. The V at which full crack occurs (which can be considered as a critical speed V_c) in each alloy is shown in Figure 3(a). Since an alloy that cracks easily even at a slow V should be highly crack susceptible, the crack susceptibility decreases in the order of alloy 800, alloy 600, alloy 625 and alloy 718.

Figure 3(b) shows the solidification cracking susceptibility of alloys 800, 600 and 625 evaluated by Fink et al. [9] using the PVR test. Bead-on-plate welding was conducted along a rectangular sheet of uniform thickness and width while the sheet was stretched in the welding direction by a crosshead that accelerated linearly during welding. The crosshead speed at which solidification cracking first occurred was taken as the critical tension speed V_{cr}. The lower the V_{cr} is, the higher the crack susceptibility. The results in Figure 3(b) are essentially consistent the TMW test results in Figure 3(a).

Figure 3(c) shows the solidification cracking susceptibility of alloys 800, 600, 625 and 718 evaluated by Lingenfelter [10] using the (longitudinal) Varestraint test. He pointed out

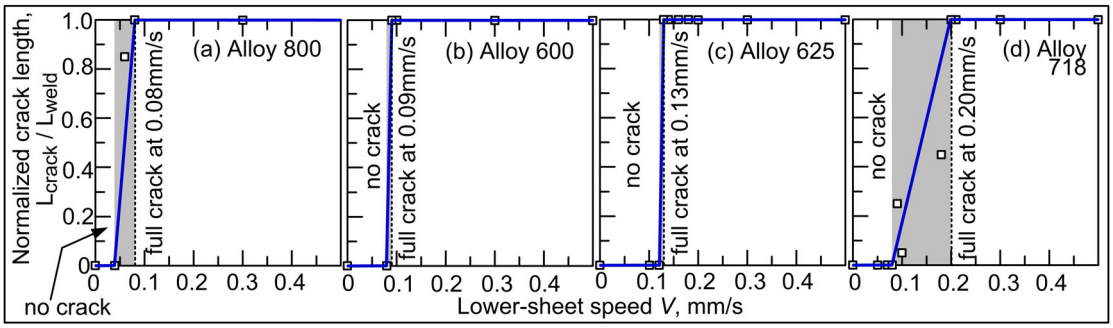

Figure 2. Results of TMW test: (a) alloy 800; (b) alloy 600; (c) alloy 625; (d) alloy 718. The shaded area indicates transition from no crack to full crack. The minimum lower-sheet speed required for full crack is indicated.

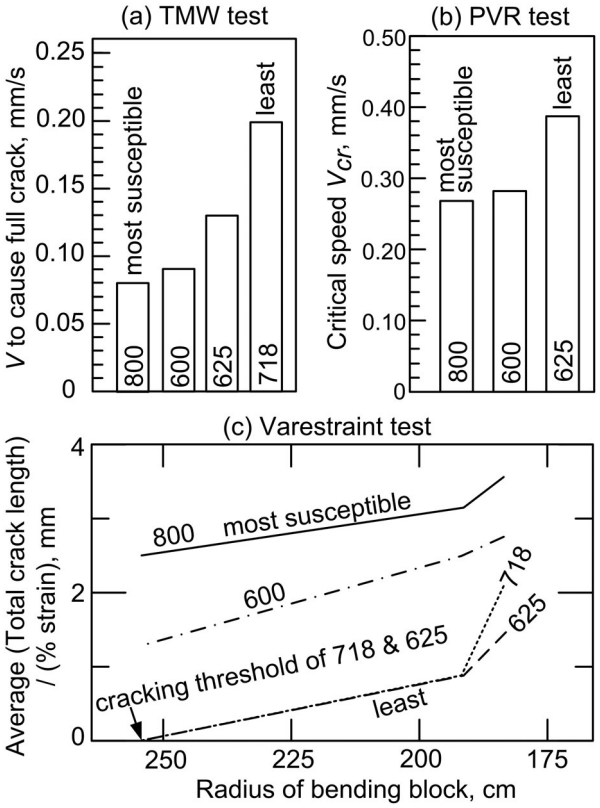

Figure 3. Crack susceptibility based on results of: (a) TMW test; (b) PVR test [9]; (c) Varestraint test [10].

> There appears to be good agreement between weldability of the Ni-Cr-Fe and Ni-Fe-Cr alloys as characterised by the Varestraint results and actual welding experience if we assume that the cracking threshold strain and cracking response at the very low strain levels are the principal indicators of hot-cracking resistance.

His test data at the low strain levels are shown in Figure 3(c). The strain was related to the radius of the bending block as follows:

$$\varepsilon = [H/(2r)] \times 100\% \quad (1)$$

where ϵ is the augmented strain induced, H the specimen thickness, and r the radius of the bending block. The threshold strain is the strain ϵ beyond which cracking occurs, that is, the bending-block radius r below which cracking occurs, e.g. about 254 cm for alloy 625 and 718 as shown in Figure 3(c).

Lingenfelter [10] further pointed out that

> Those alloys which were described as highly crack-resistant do not show cracking at the 100-in. radius block, and they show either complete absence or a very low level of cracking at the 50-in. radius block. Those alloys described as less crack resistant show increasing amounts of cracking at the 100- and 50-in. radius blocks.

Thus, based on the threshold strain and the strain at the bending-block radius of 254 cm ($\sim$100 in.) in Figure 3(c), the crack susceptibility is highest for alloy 800, lower for alloy 600, and lowest for alloys 718 and 625. Because of the unusual way the Varestraint test results were shown by Lingenfelter [10] in Figure 3(c), it is difficult to compare them with the TMW test results in Figure 3(a). However, it can be seen that both results show alloys 800 and 600 are more susceptible than alloys 718 and 625.

Crack susceptibility calculated

Figure 4 shows the curves of temperature T vs. fraction solid f_S. The arrowheads along the curves indicate the points where new solid phases start to form from the liquid phase (L) during solidification. The curves were calculated using CompuTherm's thermodynamics software Pandat [11]. The database PanNickel [12] was used for alloys 600, 625 and 718, and the database PanIron [13] for alloy 800 (which has more Fe than Ni as shown in Table 1). The Scheil solidification model was used, that is, assuming complete diffusion in liquid and no diffusion in solid [1]. The Scheil solidification model is a widely used approximation in welding and casting. Carbon is very small in quantity ($<0.06\%$ as shown in Table 1) though significant solid-state diffusion is expected. The freezing temperature range of an alloy is often used to access its susceptibility to solidification cracking, that is, the wider the range is, the higher the susceptibility [1]. Figure 4 shows the calculated freezing temperature range increases in the order of alloy 600 (130°C), alloy 718 (182°C), alloy 625 (322°C), and alloy 800 (977°C). Thus, the freezing temperature range does

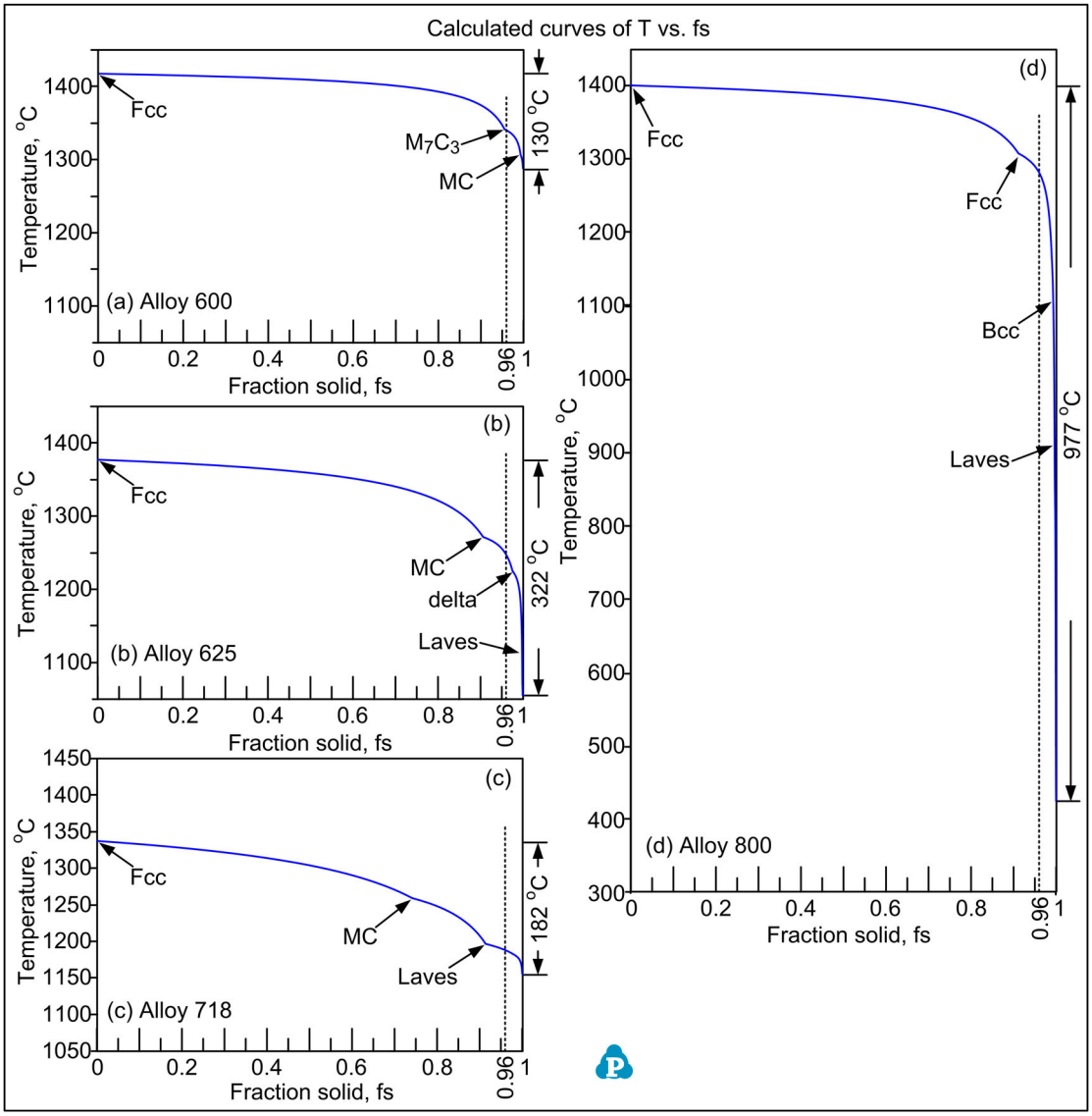

Figure 4. Curves of T vs. *fs* calculated using thermodynamics software Pandat [11]: (a) alloy 600; (b) alloy 625; (c) alloy 718; (d) alloy 800. Arrowheads along curves indicate the points where new solid phases start to from liquid L.

not correlate with the measured solidification cracking susceptibility shown in Figure 3.

Figure 5 shows the curves of T vs. $(f_S)^{1/2}$ beyond $(f_S)^{1/2} = 0.90$ based on the T-f_S curves in Figure 4. The short straight lines are the tangents showing the maximum values of $|\mathrm{d}T/\mathrm{d}(f_S)^{1/2}|$ up to $(f_S)^{1/2} = 0.98$, which are used as the index for the susceptibility to solidification cracking. The calculated susceptibility (Figure 5(e)) shows alloys 800 and 600 are equally and most susceptible. This calculation is close to the results of the TMW test (Figure 3(a)) and the PVR test (Figure 3(b)), both of which show alloy 800 is the most susceptible and alloy 600 is the next, but the difference is relatively small. The calculation of the susceptibility to solidification cracking is explained as follows.

Kou [14] proposed to use $|\mathrm{d}T/\mathrm{d}(f_S)^{1/2}|$ near $(f_S)^{1/2} = 1$ as the index for the susceptibility to solidification cracking, i.e. the higher the index is, the higher the crack susceptibility. He further showed that near $(f_S)^{1/2} = 1$, the characteristic radius of columnar dendritic grains R is proportional to the square root of the fraction solid $(f_S)^{1/2}$. So, a high $|\mathrm{d}T/\mathrm{d}(f_S)^{1/2}|$ suggests a high $|\mathrm{d}T/\mathrm{d}R|$, that is, very small lateral growth $\mathrm{d}R$ for a given temperature drop $|\mathrm{d}T|$ during cooling. Since the lateral growth is very slow, bonding between dendrites to resist lateral separation (cracking) under tension is delayed. Furthermore, since the dendrites grow longer but hardly thicker, the intergranular liquid channels become very long. Thus, the liquid feeding through the channels that is needed to resist cracking is slowed down [15]. Both the delayed bonding and the hindered liquid feeding promote cracking under tension. Kou [16] suggested using the maximum $|\mathrm{d}T/\mathrm{d}(f_S)^{1/2}|$ as the index since it occurs near $(f_S)^{1/2} = 1$. Kurz and Fisher [17] showed extensive bonding can occur between columnar dendrites at $f_S = 0.98$., i.e. $(f_S)^{1/2} = 0.99$. Since solidification cracking is unlikely once extensive bonding occurs, Kou [16] suggested using the maximum $|\mathrm{d}T/\mathrm{d}(f_S)^{1/2}|$ up to $(f_S)^{1/2} = 0.99$ as the crack susceptibility index

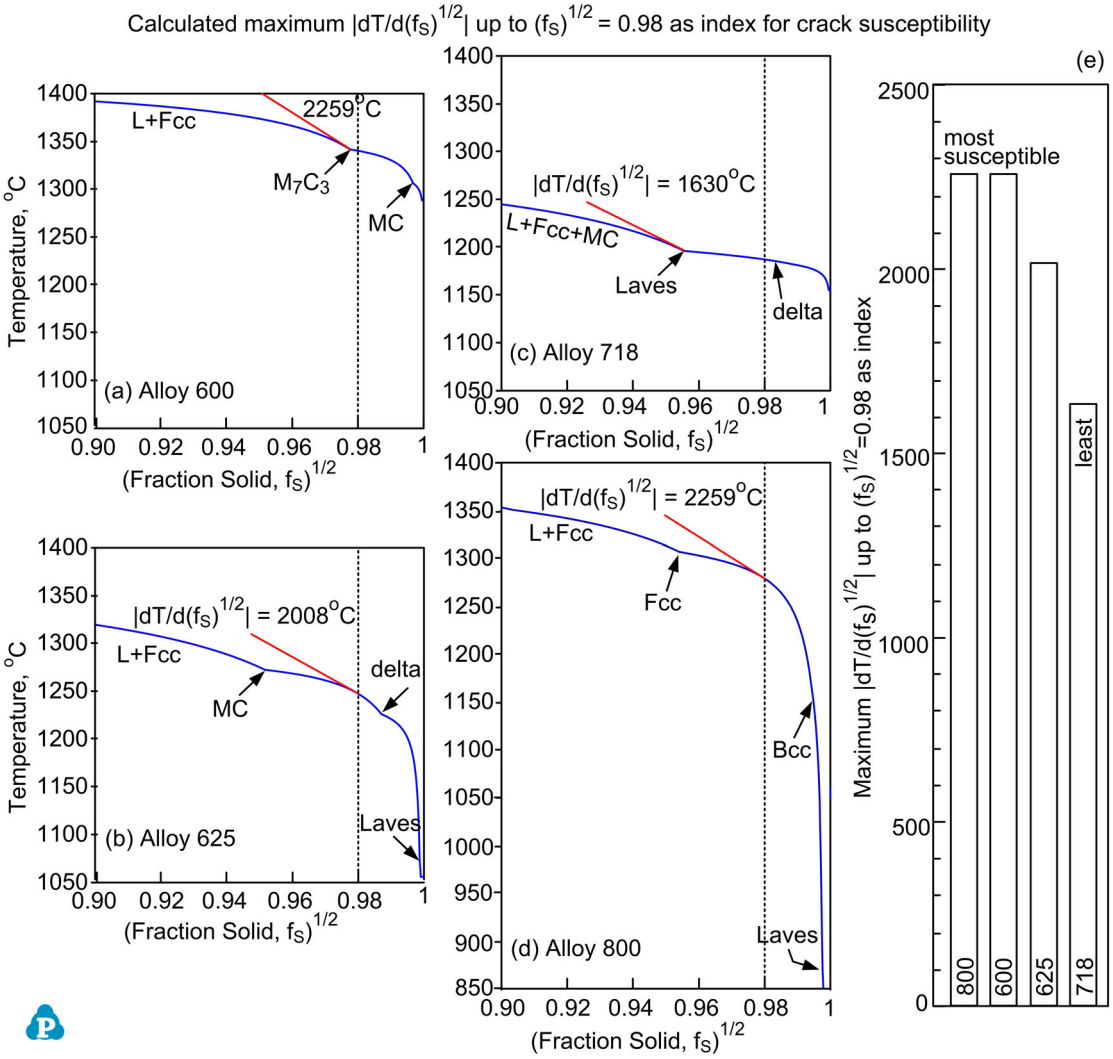

Figure 5. Maximum steepness $|dT/d(f_S)^{1/2}|$ up to $(f_S)^{1/2} = 0.98$ as index for crack susceptibility: (a) through (d) curves of T vs. $(f_S)^{1/2}$ calculated using thermodynamics software Pandat [11]; (e) susceptibility ranked.

for Al alloys. Very good agreement between calculation and testing was shown [4,16,18]. For the alloys in the present study, however, it was found that the maximum $|dT/d(f_S)^{1/2}|$ up to $(f_S)^{1/2} = 0.98$ yields better agreement with the TMW test results.

The varying resistance to solidification cracking is explained as follows based on the T-$(f_S)^{1/2}$ curves in Figure 5 and the maximum $|dT/d(f_S)^{1/2}|$ up to $(f_S)^{1/2} = 0.98$ as the index for the susceptibility to solidification cracking. A new solid phase starts to form near $(f_S)^{1/2} = 0.95$, i.e. MC in alloy 625, Laves in alloy 718 and Fcc in alloy 800. Between $(f_S)^{1/2} = 0.95$ and 0.98, the curve is very shallow in alloy 718, steeper in 625 and even steeper in alloy 800. This suggests the lateral growth of columnar dendritic grains, which causes the grains to bond together to resist cracking, is fastest in alloy 718, slower in alloy 625 and slowest in alloy 800. In alloy 600 the formation of the new solid phase has not started yet near $(f_S)^{1/2} = 0.95$. By the time M_7C_3 starts to form near $(f_S)^{1/2} = 0.98$, the curve has steepened significantly to delay the lateral growth of dendrites and hence raise the crack susceptibility of alloy 600.

The roles of carbides and the Laves phase are considered as follows. The decrease in the fraction liquid f_L and hence the increase in $(f_S)^{1/2}$ by carbides are already included in the curves of T vs. $(f_S)^{1/2}$. Thus, the possible partial blocking of liquid feeding by carbides is already considered in the crack susceptibility index. As for the Laves phase, it starts forming in alloy 718 relatively early, near $(f_S)^{1/2} = 0.95$ or $f_S = 0.90$. Thus, its presence at solidification cracks can be expected in alloy 718 as cracking, if it occurs, is before extensive bonding at $(f_S)^{1/2} = 0.98$. So, it seems debatable whether its presence can be interpreted as the evidence of the Laves phase causing solidification cracking in 718. Also, higher cooling rates result in finer dendrites and hence finer interdendritic Laves, but they also result in a smaller mushy zone with faster dendrite growth to cause bonding and less tension (thermally induced) to separate dendrites. So, it may also be debatable if solidification cracking is actually reduced by a finer Laves-phase distribution. Further investigation may help clarify the roles of carbides and the Laves phase in solidification cracking in Ni-base alloys.

Critical local strain rate estimated

Figure 6 shows the transverse cross-section of the alloy 800 weld that started to crack fully at $V = 0.08$ mm/s. The macrograph shows the overall width at the top surface of the weld W is 7.3 mm. In the TMW test the moving lower sheet causes the lower-sheet weld edge to move away from the stationary upper-sheet weld edge at V. Thus, the nominal strain rate across the fusion zone can be approximated as $V/W = 0.011\ s^{-1}$ ($= 0.08\ mm\ s^{-1}$ divided by 7.30 mm). Cracking initiates near the triple junction between the fusion zone, the upper sheet, and the lower sheet. The dotted lines in Figure 6(b) indicate the region containing cracks, up to about two-thirds of the total crack path to the weld top surface. Cracking appear to concentrate within the region instead of spreading throughout the fusion zone. The average width of the region is estimated as $R \approx 403\ \mu m$, and the average width of the main open crack $C \approx 122\ \mu m$. So, the width of the region under high local tension just before cracking occurs is estimated as $D \approx 281\ \mu m$ ($= 403 - 122\ \mu m$). The local critical strain rate can be taken as V/D as an approximation [5]. Thus, $V/D \approx 0.285\ s^{-1}$ ($0.08\ mm\ s^{-1}$ divided by 0.281 mm). Since the measurements of R and D are done rather arbitrarily, the critical local strain rate can only be considered as a rough estimation.

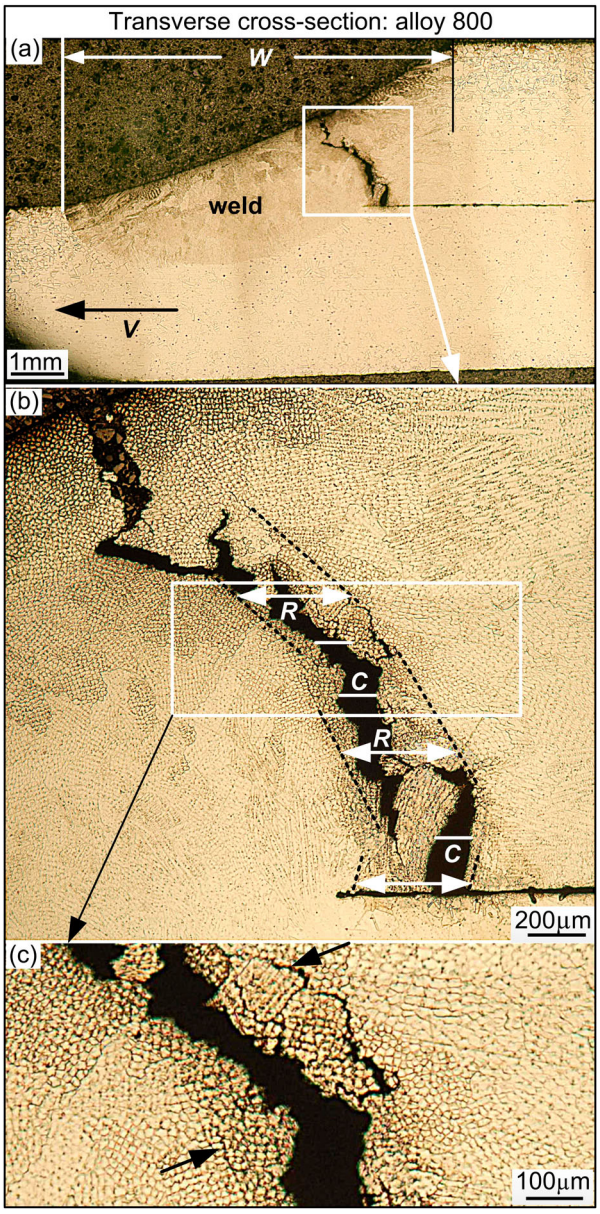

Figure 6. Transverse cross-section of weld of alloy 800 tested at $V = 0.08\ mm\ s^{-1}$: (a) macrograph ($W = 7.3$ mm); (b, c) micrographs. *R*: width of region with cracking, *C*: width of main open cracks.

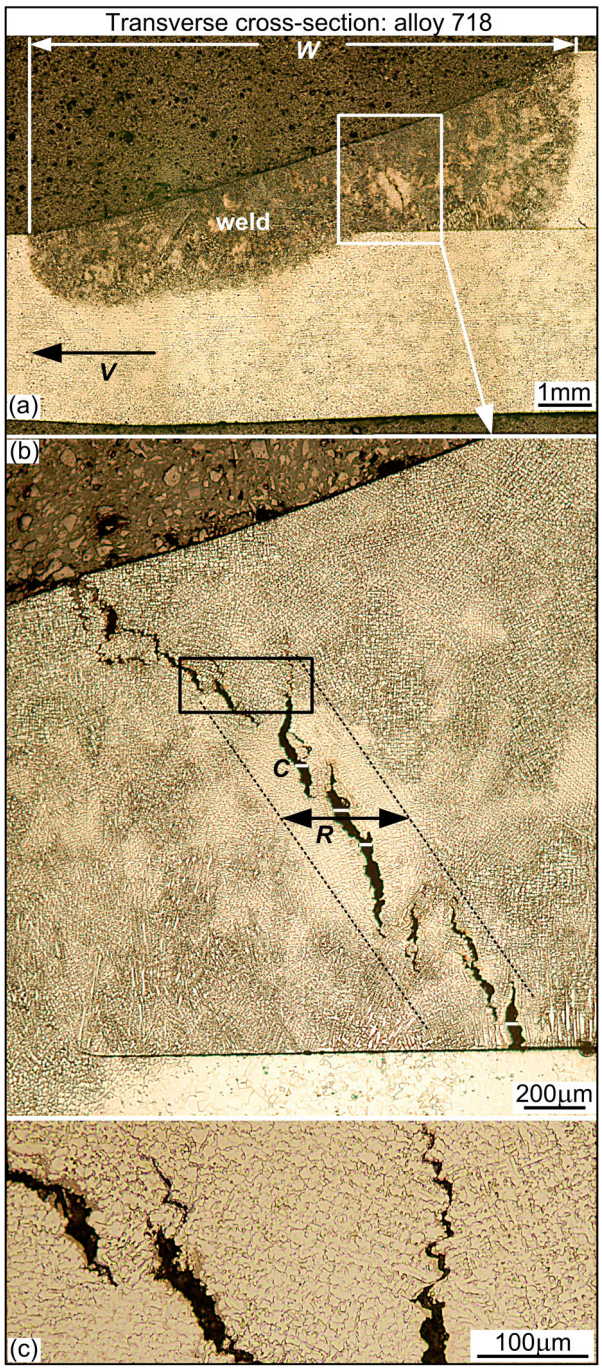

Figure 7. Transverse cross-section of weld of alloy 718 tested at $V = 0.20\ mm\ s^{-1}$: (a) macrograph ($W = 10.4$ mm); (b, c) micrographs.

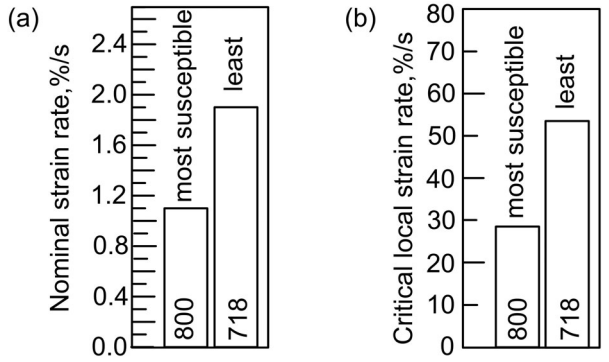

Figure 8. Strain rates estimated for welds of alloy 800 in Figure 5 and alloy 718 in Figure 6: (a) nominal strain rate across weld width, (b) critical local strain rate near crack.

Similar results are shown in Figure 7 for the alloy 718 weld that started to crack fully at $V = 0.20\,\text{mm s}^{-1}$. The macrograph of the weld shows the overall width of the weld at its top surface W is 10.4 mm. The nominal strain rate can be approximated as $V/W = 0.019\,\text{s}^{-1}$ ($0.20\,\text{mm s}^{-1}$ divided by 10.4 mm). As shown, $D \approx 374\,\mu\text{m}$ ($= 419 - 45\,\mu\text{m}$). Thus, the local critical strain rate can be taken as $V/D \approx 0.535\,\text{s}^{-1}$ ($0.20\,\text{mm s}^{-1}$ divided by 0.374 mm). Figure 8 compares the strain rates in the two welds. As shown, the critical local strain rate is much higher than the nominal strain rate in both cases. This suggests the strain rate is not uniform in the fusion zone but highly localised. Furthermore, the critical local strain rate is significantly higher for alloy 718 than for alloy 800, that is, it takes a significantly higher local strain rate to initiate solidification cracking in 718 than 800. This is consistent with the significantly lower crack susceptibility of 718 than 800 as shown in Figure 3(a) by the TMW test.

Conclusions

1. The TMW test can be applied to Ni-base alloy to evaluate their susceptibility to solidification cracking.
2. The results of the TMW test show the susceptibility to solidification cracking decreases in the order of alloy 800, alloy 600, alloy 625 and alloy 718. The relative ranking of the susceptibility is essentially consistent with those based on the PVR test and the Varestraint test.
3. The index for the solidification cracking susceptibility, i.e. the maximum $|\text{d}T/\text{d}(f_S)^{1/2}|$ near $(f_S)^{1/2} = 1$, shows a crack susceptibility ranking similar to that based on the TMW test.
4. The critical local strain, estimated based on the transverse micrograph and the lower-sheet speed causing full cracking in the TMW test, is significantly higher for alloy 718 than alloy 800. This is consistent with the significantly lower crack susceptibility of 718 than 800 shown by the TMW test.

Acknowledgements

Chunzhi Xia was supported by the Jiangsu Overseas Visiting Scholar Program for University Prominent Young & Middle-aged Teachers and Presidents as a visiting professor at the University of Wisconsin–Madison from 2018 to 2019. Sindo Kou was supported by the National Science Foundation initially under grant number DMR 1500367 and subsequently under grant number DMR1904503.

Disclosure statement

No potential conflict of interest was reported by the author(s).

Funding

Chunzhi Xia was supported by the Jiangsu Overseas Visiting Scholar Program for University Prominent Young & Middle-aged Teachers and Presidents as a visiting professor at the University of Wisconsin–Madison from 2018 to 2019. Sindo Kou was supported by the National Science Foundation (US) initially under grant number DMR 1500367 and subsequently under grant number DMR1904503.

References

[1] Kou S. Welding metallurgy. 3rd ed. Hoboken (NJ): Wiley; 2020.
[2] Soysal T, Kou S. A simple test for solidification cracking susceptibility and filler metal effect. Weld J. 2017;96(10):389s–401s.
[3] Soysal T, Kou S. Effect of filler metals on solidification cracking susceptibility of Al alloys 2024 and 6061. J. Mater. Proc. Tech. 2019;266:421–428.
[4] Soysal T, Kou S. A simple test for assessing solidification cracking susceptibility and checking validity of susceptibility prediction. Acta Mater. 2018;143:181–197.
[5] Soysal T, Kou S. Role of liquid backfilling in reducing solidification cracking in aluminum welds. Sci Technol Weld Joining. 2020;25(5):415–421.
[6] Liu K, Kou S. Susceptibility of magnesium alloys to solidification cracking. Sci Technol Weld Joining. 2020;25(3):251–257.
[7] Liu K, Yu P, Kou S. Susceptibility of stainless steels to solidification cracking: new test and explanation. Weld J. 2020.
[8] Savage WF, Lundin CD. The Varestraint test. Weld J. 1965;44(10):433s–442s.
[9] Fink C, Zinke M, Keil D. Evaluation of hot cracking susceptibility of nickel-based alloys by the PVR test. Weld World. 2012;56(7-8):37–43.
[10] Lingenfelter AC. Varestraaint testing of nickel alloys. Weld J. 1972;51(9):430s–436s.
[11] Pandat. Phase diagram calculation software package for multicomponent systems. Madison (WI): Computherm LLC; 2019.
[12] PanNickel. Thermodynamic database for commercial nickel alloys. Madison (WI): Computherm LLC; 2019.
[13] PanIron. Thermodynamic database for commercial iron alloys. Madison (WI): Computherm LLC; 2019.

[14] Kou S. A criterion for cracking during solidification. Acta Mater. 2015;88:366–374.
[15] Kou S. Transport phenomena and materials processing. Hoboken (NJ): Wiley; 1996.
[16] Kou S. A simple index for predicting the susceptibility to solidification cracking in welding. Weld. J. 2015;94(12):374s–388s.
[17] Fisher DJ, Kurz W. Unpublished Research. Switzerland: Department of Materials, EPFL-Swiss Institute of Technology Lausanne; 1978.
[18] Soysal T, Kou S. Predicting the effect of filler metals on solidification cracking susceptibility of Al alloys 2024 and 6061. Sci Technol Weld Joining. 2019;24(6):559–565.